

Laser-induced thermal desorption analysis of the surface during Ge etching in a Cl₂ inductively coupled plasma

Jae Young Choe and Irving P. Herman^{a)}

Department of Applied Physics and Columbia Radiation Laboratory, Columbia University, New York, New York 10027

Vincent M. Donnelly

Bell Laboratories, Lucent Technologies, Murray Hill, New Jersey 07974

(Received 23 June 1998; accepted 21 August 1998)

Laser desorption laser-induced fluorescence (LD-LIF) detection of GeCl was used to determine *in situ* the surface coverage of chlorine during the etching of germanium by Cl₂ in an inductively coupled plasma (ICP) reactor. The ICP operated in the dim mode for radio frequency (rf) power $\lesssim 350$ W and in the bright mode for higher powers. The etch rate was 3.5 $\mu\text{m}/\text{min}$ with 540 W rf power and -40 V substrate bias. The chlorine surface coverage was about $2\times$ that with chlorine flow only and the plasma off, both with dim- and bright-mode operation, and was independent of rf power within each mode for laser repetition rates of 0.2, 5, and 15 Hz. Similarly, the chlorination of the adlayer did not change when the ion energy was increased from 16 to 116 eV by increasing the substrate bias voltage, both with dim- and bright-mode operation. This was confirmed by x-ray photoelectron spectroscopy measurements in a similar high density reactor, where it was found that the surface density of chlorine was $\sim 2.6\times 10^{15}$ Cl/cm². As the ion energy increases from 16 to 116 eV, the etch yield of ions increases from 1 to 3 atoms/ion. "Wait and probe" measurements show that the GeCl_x adlayer is quite stable. Since the same adlayer chlorine content was measured by LD-LIF under high ion current/fast etch conditions (bright mode) and low ion current/slow etch conditions (dim mode), both the adlayer chlorine content and the etch rate seem to be controlled by the ion current to the wafer. Previously reported work in Si etching in this ICP [J. Vac. Sci. Technol. A 15, 3024 (1997)] showed a similar independence of adlayer chlorination with rf power, but much slower chlorination and an increasing chlorination of the adlayer with increasing ion energy. © 1998 American Vacuum Society. [S0734-2101(98)05006-4]

I. INTRODUCTION

Plasma etching of Ge is of interest, in part, because of the need to pattern devices composed of GeSi alloys. While there have been several studies on the rate of etching Ge and GeSi by plasmas,¹⁻⁸ the fundamental understanding of such processes is much less complete than that for Si etching. Since the competitive balance of adlayer formation and removal determines the etch rate, *in situ* measurement of the adlayer itself is important in understanding the etching process. Previous studies of Si etching by high density chlorine plasmas⁹⁻¹¹ showed that laser desorption (LD) of the adlayer by a XeCl excimer laser followed by laser-induced fluorescence (LIF) of major desorbing species provides a semiquantitative measure of the degree of halogenation of the surface layer. In particular, the LD-LIF intensity of SiCl, a major desorbing species during the etching of Si by Cl₂ in inductively coupled and helical resonator high density plasmas, was found to be proportional to the adlayer chlorination SiCl_x; analogous LD-LIF measurements of desorbed SiBr during plasma etching by HBr and HBr/Cl₂ mixtures were used to determine the bromination of the adlayer.¹² In this article we explore the use of LD-LIF of desorbed GeCl to analyze the GeCl_x surface adlayer during the etching of Ge in a chlorine inductively coupled plasma (ICP) reactor. Dis-

tinct similarities and differences in the chlorination of the adlayer are found during steady-state ICP etching of Ge and Si under various process conditions.

II. EXPERIMENTAL METHODS

The ICP chamber is made of a 6 in. stainless steel cube where one of four side ports is used for light collection. The source is powered by a 13.56 MHz rf power generator through an impedance matching network and a water-cooled four-turn "stove-top" coil above the rf coupling quartz window, which serves as the top port of the plasma chamber. The sample holder was rf biased at 18 MHz to induce the negative dc bias voltage that controls the ion bombardment energy. More details about this reactor are provided elsewhere.¹¹ For rf powers below about 350 W, the ICP operates in the capacitively coupled dim mode, while at higher powers it operates in the inductively coupled bright mode. Cl₂ was flowed at a rate of 25 sccm, leading to an 18 mTorr pressure at the wafer. Measurements of ion density and electron temperature in this ICP, made using a retractable Langmuir probe with the sample stage removed, have been reported previously.¹¹

The germanium sample used for laser desorption and etch rate measurements was cleaved from an *n*-type (100) (antimony doped, $<0.4 \Omega \text{ cm}$) wafer. It was mounted on a 2 in. diam Si wafer that was itself bonded to the sample holder

^{a)}Electronic mail: iph1@columbia.edu

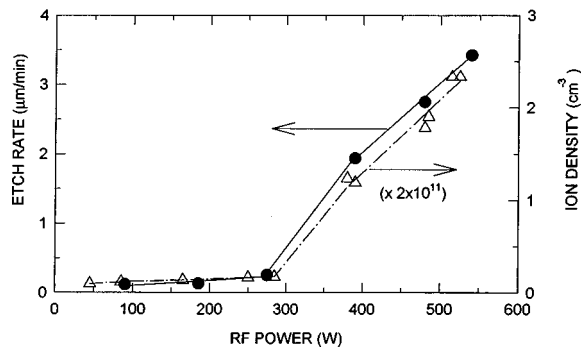


FIG. 1. Etch rate of Ge (●) and ion density (Δ) vs rf power (18 mTorr Cl_2 , -40 V dc substrate bias).

using indium. This sample was positioned 3.8 cm below the rf coupling window, and was maintained at room temperature by circulating water. For the etch rate measurements, the Ge sample was first patterned with photoresist (Shipley S1818); after etching, the etched depth was measured by profilometry following photoresist stripping (EKC J100 solution).

In the LD-LIF experiments, pulses from a XeCl excimer laser (Questek 2440, 308 nm, ~ 20 ns long pulses) were focused by a 50 cm focal length quartz lens, and directed onto the Ge sample at normal incidence. This same laser both heated the sample, to induce thermal desorption of surface-adsorbed species, and excited laser-induced fluorescence in those desorbed species that absorb at 308 nm. Since the XeCl laser excites the $\text{GeCl } B^2\Sigma \leftarrow X^2\Pi_r$ transition, this method is sensitive to GeCl, which is expected to be a major desorbing species. Given the laser pulse width (20 ns) and collision time in the plasma, the laser detects LIF in desorbing GeCl molecules before they can suffer collisions. The 308 nm laser induces resonant excitation in both $\text{GeCl } B^2\Sigma \leftarrow X^2\Pi_r$ subsystems,^{13–16} specifically, $v' = 1, 2 \leftarrow v'' = 3, 4$ in the first subsystem ($r = 3/2$) and $v' = 0, 1 \leftarrow v'' = 4, 5$ in the second subsystem ($r = 1/2$). The emission was collected, analyzed by a monochromator, and detected by a GaAs photomultiplier. This signal was analyzed with a boxcar integrator. With typical pulse energy of 28 mJ and spot size of $4.5 \text{ mm} \times 3 \text{ mm}$ (13.5 mm^2), the fluence at the sample surface was $\sim 0.2 \text{ J/cm}^2$. As will be described, nearly all of the reacted adlayer is removed using this fluence for the different processing conditions studied, and therefore the LD-LIF signal is expected to be proportional to the chlorine content of the adlayer.

III. RESULTS

Figure 1 shows the etch rate as a function of rf power at a fixed pressure (18 mTorr) and dc substrate bias (-40 V). In dim-mode operation, the etch rate increases slowly from $0.1 \mu\text{m/min}$ at 90 W to $0.25 \mu\text{m/min}$ at 275 W. It is an order of magnitude higher with bright-mode operation, increasing from $2.0 \mu\text{m/min}$ at 400 W to $3.4 \mu\text{m/min}$ at 540 W. The

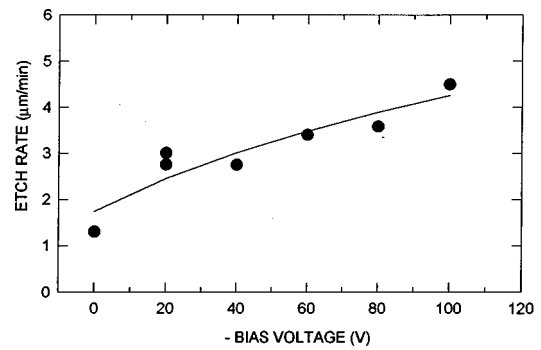


FIG. 2. Etch rate of Ge vs dc substrate bias (18 mTorr Cl_2 , 480 W rf power, bright mode).

etch rate also increases with increasing dc substrate bias, from $1.3 \mu\text{m/min}$ with no applied bias to $4.5 \mu\text{m/min}$ with -100 V bias at 480 W (Fig. 2).

The plasma-induced emission (PIE) [optical emission (OE)] spectrum during steady-state germanium etching in the Cl_2 ICP is shown in Fig. 3. It has many very strong emission lines from atomic Ge, strong GeCl emission bandheads due to $A' \ ^2\Delta \rightarrow X^2\Pi_r$, near 339.27 nm for the second subsystem and 350.15 nm for the first subsystem, and weak GeCl emission $B^2\Sigma \rightarrow X^2\Pi_r$ band transitions from 289.12 to 309.80 nm. The wafer was lowered to 4 cm below the rf coupling window for these PIE measurements only, and the PIE was measured 0.2 cm above the wafer.

The LD-LIF spectrum during Ge etching in the Cl_2 plasma, shown in Fig. 4, has GeCl molecular emission bands in both $B^2\Sigma \rightarrow X^2\Pi_r$ subsystems, which are identified in Fig. 4. Strong Ge emission lines are also seen and are attributed to a transient increase in PIE after laser desorption (LD-PIE). Figure 5 shows the time dependence of the LD-LIF of the GeCl peak at 297.12 nm and the LD-PIE of the Ge peak at 265.17 nm. The Ge LD-PIE emission line at 265.17 nm persisted for 10–15 μs after laser desorption, which is consistent with the rate of diffusion of the transient increase in density after LD to regions outside the region of light collection.⁹ In contrast, the GeCl LD-LIF emission decreased rapidly after laser desorption, which is expected for LD-LIF of species that are excited by the laser and that radiatively decay fast. In subsequent experiments, the LD-LIF intensity

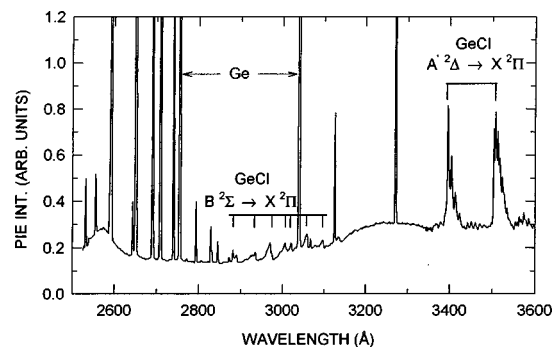


FIG. 3. Spectrum of steady-state PIE during Ge etching (18 mTorr Cl_2 , 500 W rf power, bright mode, 0 V dc bias).

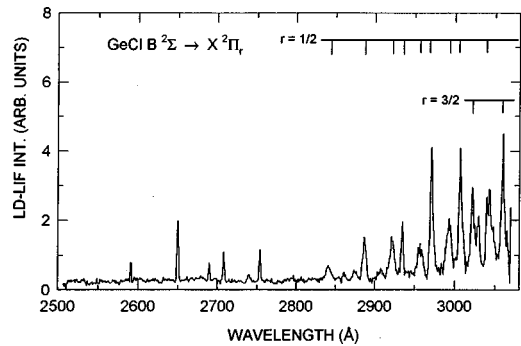


FIG. 4. LD-LIF spectrum showing the GeCl $B \rightarrow X$ transition (18 mTorr, Cl_2 , 490 W rf power, bright mode, -32 V dc bias). There is a background of Ge transitions due to a transient enhancement in the PIE signal from the laser desorption (LD-PIE). Background laser scattering has been subtracted.

was monitored as a function of plasma conditions using the 289.12 nm GeCl emission line. A transmission filter centered at 290 nm was placed in front of the monochromator to reject scattered laser light. Still, some scattered light is detected; it has been subtracted from the spectrum shown in Fig. 4.

Figure 6 shows a typical trace of LD-LIF as the ICP was alternately turned on and off, with a different value of the rf power delivered to the coil for each "on" phase. The substrate bias voltage was -40 V and the laser repetition rate was 5 Hz. The letters D and B represent dim-mode and the bright-mode operation, respectively. These results are summarized in Fig. 7. The LD-LIF intensity is seen to vary little when the rf power is varied above ~ 50 W. This same LD-LIF intensity and insensitivity to rf power (down to 100 W) was also seen using 0.2 and 15 Hz laser repetition rates. LD-LIF was also measured as the ICP was alternately turned on and off, with a different value of substrate bias voltage for each on phase, as shown in Fig. 8. The rf power to the ICP source was 485 W (bright mode) in Fig. 8(a) and 150 W (dim mode) in Fig. 8(b), and the laser repetition rate was 5 Hz. The results are summarized in Figs. 9(a) and 9(b), respectively. The LD-LIF intensity varies little with changing substrate bias voltage, both for dim- and bright-mode operation. Survey measurements at other GeCl $B \rightarrow X$ emission

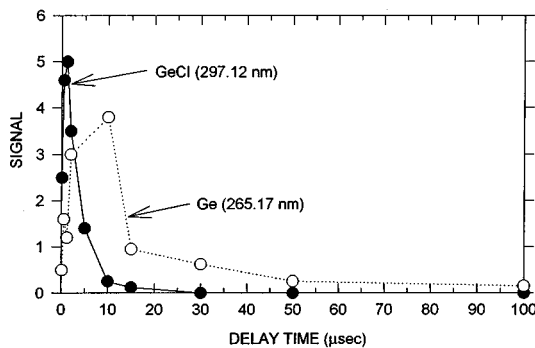


FIG. 5. LD-LIF intensity of the 297.12 nm GeCl $B \rightarrow X$ emission line and the transient LD-PIE intensity of the 265.17 nm Ge emission line vs delay time of the boxcar integrator (18 mTorr, 480 W rf power, bright mode, 0 V bias).

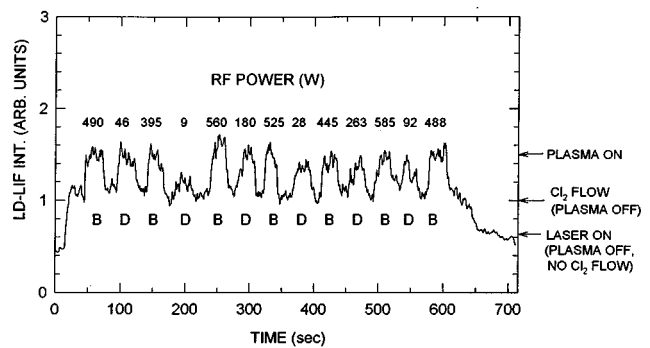


FIG. 6. Trace of the LD-LIF GeCl intensity at 289.12 nm as the plasma was turned on and off vs time, with the different rf powers during each on cycle (18 mTorr, -40 V dc bias). The letter D indicates dim-mode operation, while B indicates bright-mode operation. The laser repetition rate was 5 Hz.

bands, including 297.12 nm, gave very similar results to these reported at 289.12 nm.

"Wait and probe" experiments were conducted to examine the stability of the chlorinated adlayer and to determine what fraction of the surface adlayer is removed per laser pulse from the targeted spot. In these tests, the laser first irradiates the Ge surface under steady-state conditions, with the Cl_2 plasma turned on (or with the plasma off, but with exposure to Cl_2). After the LD-LIF signal intensity is noted, the laser is blocked, and then after several seconds the plasma (if on) is turned off and the chlorine flow is stopped; the chamber is then pumped for several minutes. The laser pulse train is then allowed to irradiate the surface again. This was performed with the ICP operating in the bright mode with either low (0 V) or high (-100 V) bias, and with chlorine exposure only. Based on earlier experiments on etching of Si in an ICP reactor,¹¹ these three cases represent conditions with potentially different levels of adlayer chlorination and different surface binding energies. In each case, when the laser pulses again irradiated the Ge surface after the chamber was pumped, the first pulse produced a LD-LIF signal with an intensity approximately equal to the steady-state value, which indicates that the chlorinated layer is stable during pumpdown. The second pulse (and subsequent pulses) produced a much smaller signal at the background laser scatter level, which indicates that each laser pulse re-

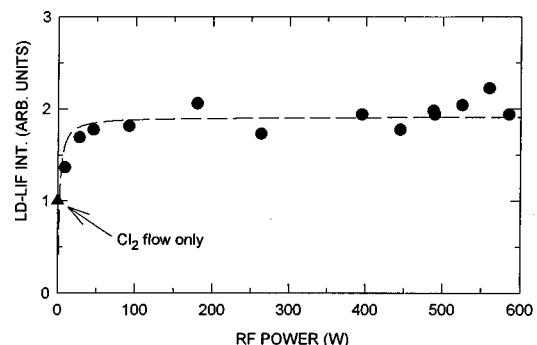


FIG. 7. LD-LIF intensity vs rf power from Fig. 6, normalized by the LD-LIF signal during Cl_2 flow with the plasma off.

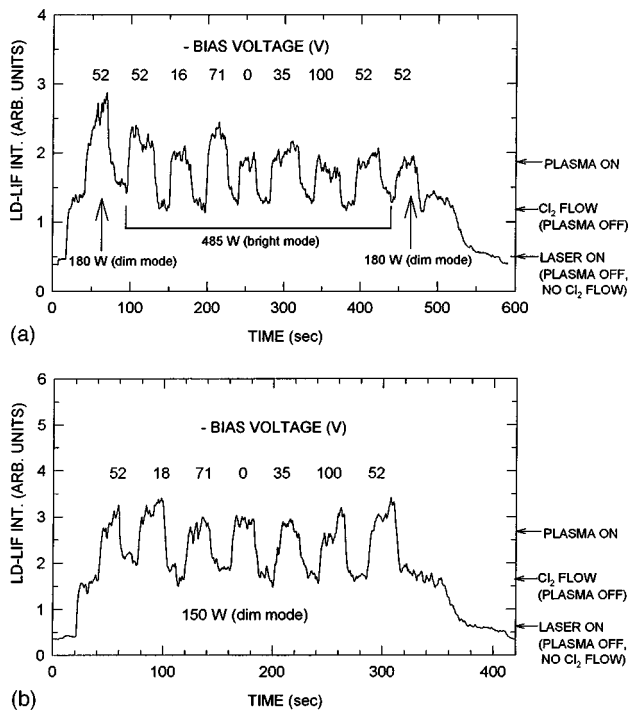


Fig. 8. (a) Trace of the LD-LIF GeCl intensity at 289.12 nm as the plasma was turned on and off vs time, with the different dc biases during each bright-mode on cycle (18 mTorr, 5 Hz laser repetition rate). For comparison, the first and last cycles were with dim-mode operation. The magnitude of bias is indicated above each cycle. (b) Similar run as (a) but with dim-mode operation.

moves most (if not all) of the adlayer from the targeted spot (saturation) with the laser fluence used here. Figure 10 shows a wait and probe experiment with 480 W rf power for medium bias voltage (-40 V).

X-ray photoelectron spectroscopy (XPS) measurements were conducted to check the unexpected independence of the LD-LIF signal on ion energy. Ge samples were etched in a helical resonator (HR) plasma operating at 18 mTorr Cl_2 and 500 W, and were then transferred (in vacuum) to an attached XPS analysis chamber. Previous etch rate and LD-LIF studies of plasma etching of Si (Ref. 11) have shown that this HR and the ICP (used for all of the other reported work) have similar plasma conditions and etching parameters. The wait and probe experiments demonstrate that the GeCl_x adlayer is stable during the vacuum transfer. After Ge etching, XPS determined that the Cl/Ge ratio at the surface is $0.455 (\pm 0.015)$, $0.455 (\pm 0.005)$, and $0.50 (\pm 0.03)$ for 40, 117, and 170 eV ion energies, respectively. These correspond to areal densities of $2.6 (\pm 0.1) \times 10^{15}$, $2.6 (\pm 0.1) \times 10^{15}$, and $2.8 (\pm 0.2) \times 10^{15}$ Cl/cm² in the adlayer, respectively. (The stated errors for areal densities do not include the roughly 50% uncertainty in the electron mean free path lengths.)

IV. DISCUSSION

A. Analysis of observations

The strong GeCl LD-LIF signals suggest that GeCl is a major laser desorption product of Ge surfaces exposed to Cl_2

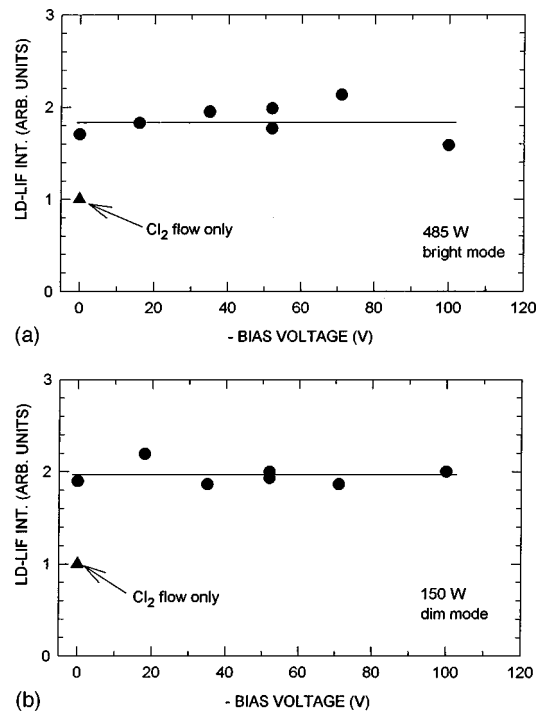


Fig. 9. (a), (b) LD-LIF intensity vs dc substrate bias from Figs. 8(a) and 8(b), respectively. The intensity during the plasma on cycle was normalized by that with Cl_2 flow and the plasma off.

plasmas. The laser excites LIF in desorbing molecules before they can be dissociated by electron impact. Therefore, the observed signal is not due to GeCl LD-PIE, which could originate from the electron-induced dissociation and concomitant or subsequent electron excitation of desorbing GeCl_2 . The authors of Ref. 17 suggest that Ge(100) surface dimers exposed to a Cl_2 beam in ultrahigh vacuum are saturated with one full monolayer of Cl as the monochloride (and not the dichloride). XPS measurements by Zhang *et al.* show that GeCl is also a major surface component during Ge etching in chlorine based plasma.⁵ The GeCl LD-LIF signal appears to represent the degree of surface adlayer chlorination.

While GeCl_2 cannot be detected with the current LIF system, it cannot be discounted as a desorption product because it is seen after thermal etching of Ge. Madix and Schwarz

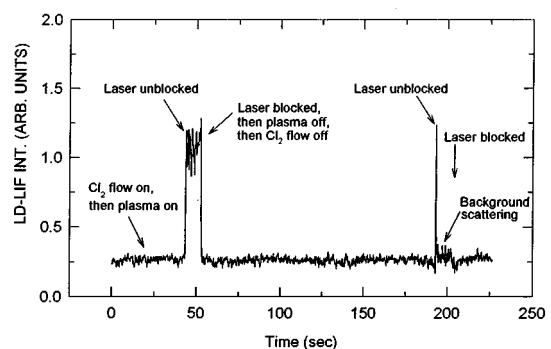


Fig. 10. Wait and probe measurement of LD-LIF GeCl intensity at 297.12 nm (480 W rf power, -40 V bias, 5 Hz laser repetition rate).

concluded that GeCl_2 is the only desorption product during the thermal etching of Ge by a modulated Cl_2 beam.¹⁸ Temperature-programmed desorption of GeCl_2 from a Ge surface exposed to HCl gas was described by near-first-order kinetics.¹⁹ In Ref. 20 it was concluded that GeCl_2 is the only product during laser-induced etching of Ge by a supersonic Cl_2 beam. Because of the ion-induced damage on the surface during plasma etching, lower chlorides can be desorbed during plasma exposure, as has been seen for Si etching.

The Ge surface is roughly twice as chlorinated during ICP etching as during exposure to chlorine, with the plasma off (Fig. 7). A more heavily chlorinated adlayer during plasma etching has also been seen for Si.¹¹ If the chlorine content of the Ge surface during exposure to Cl_2 gas flow is 1 monolayer (ML), these LD-LIF measurements suggest that the chlorine content of the surface is ~ 2 ML when the plasma is on. The degree of surface chlorination during Ge etching is relatively insensitive to rf power (Fig. 7) for a 5 Hz laser repetition rate. It is approximately the same for rf powers from 50 W (dim-mode operation) to 500 W (bright-mode operation), even though the ion density increases from $2 \times 10^{10}/\text{cm}^3$ to $4 \times 10^{11}/\text{cm}^3$ in this range.¹¹ This general insensitivity of the adlayer content to rf power was also observed in previous studies of ICP etching of Si.¹¹ Below 50 W there is a falloff in the content of the GeCl_x adlayer.

The etch rate of Ge in the chlorine ICP reactor is faster than that for Si under comparable plasma conditions. In bright-mode operation it is about $2.5 \times$ faster (2750 vs 1100 nm/min at 480 W rf power and -40 V bias), and in the dim mode it is about $3 \times$ faster (300 vs 90 nm/min at 300 W rf power and -40 V bias). Fast etching in Ge has been previously reported³⁻⁵ in low density plasmas; larger etch rates for Ge *vis-à-vis* Si have also been reported in chlorine-based plasmas,³⁻⁶ as well as in fluorine-^{1-4,7} and bromine-based plasmas.^{3,4} The LD-LIF signal was noticeably smaller during Si etching with dim-mode operation when the laser repetition rate was 5 Hz than when it was 0.2 Hz,¹¹ suggesting that the surface chlorination does not attain steady state in the dim mode in 0.2 s (5 Hz) because of the low ion density (2×10^{10} ions/ cm^3). In bright-mode operation (4×10^{11} ions/ cm^3), the LD-LIF signals were the same for Si at both repetition rates. However, during Ge etching there is almost no variation of the LD-LIF signal at any rf power >100 W when the laser repetition rate is varied between 0.2 and 15 Hz. This suggests that the surface is rechlorinated very rapidly (<0.1 s) to the saturation level during Ge etching even with the very low ion density typical of dim-mode operation. Furthermore, since the etch rate closely follows the ion density variation with rf power (Fig. 1), while the adlayer thickness does not change, increasing the ion flux equally increases the rate of adlayer formation (chlorination) and adlayer removal (etching) for Ge etching; this had previously been noted for Si etching.¹¹

The content of the chlorinated adlayer is also insensitive to the dc substrate bias during Ge etching for substrate biases ranging from 0 to -100 V, corresponding to ion energies ranging from approximately 16–116 eV (using the 16 V

plasma potential measured in Ref. 11). In contrast, the chlorine content of the surface increases over the same dc bias range during Si etching. Increasing ion energy (1) leads to deeper penetration of chlorine into the subsurface in Si but not in Ge, (2) causes such changes for both Si and Ge but they are not seen by LD-LIF detection of desorbed GeCl , or (3) is not important in Ge because there is already deep penetration of thermal chlorine atoms or neutralized low-energy ions.

The XPS measurements after Ge etching in a chlorine HR plasma showed that the areal density of chlorine remained essentially constant $\sim 2.6 \times 10^{15}$ Cl/ cm^2 from 40 to 117 eV (nearly overlapping the range of the LD-LIF ICP measurements) and increased slightly to $\sim 2.8 \times 10^{15}$ Cl/ cm^2 at 170 eV.²¹ This rules out possibility (2) and confirms the conclusions of the LD-LIF measurements. In contrast, during Si etching in the HR, the areal density of chlorine increased from 1.8×10^{15} Cl/ cm^2 at 40 eV to 2.3×10^{15} Cl/ cm^2 at 170 eV, which was also seen in LD-LIF measurements.¹¹ The Ge surface is more heavily chlorinated than the Si surface at low bias energies. Increased penetration of neutralized Cl^+ or Cl_2^+ ions into Ge subsurfaces with larger ion energy, and subsequent chlorination of the subsurface, may be less important in Ge than in Si, possibly because there is more ion penetration in Ge at low ion energy. Higher ion energy may equally increase sputtering and chlorination of the adlayer on Ge.

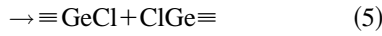
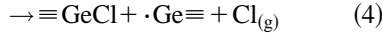
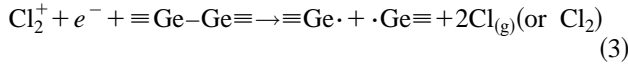
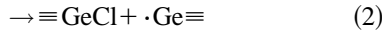
Using XPS, Zhang *et al.* concluded that the adlayer on the Ge surface (~ 5 Å) is slightly thicker than that on the Si surface (~ 3 Å) when Ge and Si samples are, respectively, etched in chlorine-based reactive-ion etching (RIE) reactors.⁵ The results of Ref. 22 suggest that for the self-bias voltage of -190 V in Ref. 5 the chlorine content of the Si surface should be $\sim 3 \times 10^{15}$ Cl/ cm^2 , which is equivalent to a SiCl_x thickness of ~ 15 Å. Zhang *et al.* estimated a much thinner adlayer.

B. Etching mechanism

Oehrlein and co-workers have concluded that germanium etching in chlorine plasmas is ion enhanced on the basis of the variation of etch rate with pressure.⁴ Vallon *et al.* studied the profile of masked Si/Ge bilayers etched in a high-density-plasma helicon source using a $\text{Cl}_2/\text{O}_2/\text{He}$ gas mixture.²³ They found the etching profile to be nearly anisotropic and concluded that Ge etching is ion assisted in chlorine plasmas. They attributed the small amount of lateral etching they saw to spontaneous etching of the Ge sidewalls by oxygen. It is well known that Si etching is ion enhanced in Cl_2 plasmas.

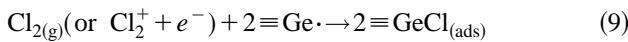
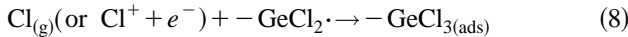
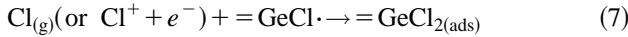
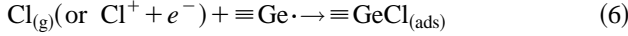
The elementary steps of etching of Ge by Cl_2 plasmas are expected to be similar to those for Si etching; representative steps are listed below: (I) reactions (1)–(5): Cl^+ and Cl_2^+ ions can create additional adsorption sites near the surface and in the process can concomitantly chlorinate the surface, (II) reactions (6)–(9): neutral chlorine (Cl and Cl_2) and chlorine ions (Cl^+ and Cl_2^+) can chlorinate these and other sites, and (III) reactions (10)–(17): ions can sputter surface-bound GeCl_x .

Ion-induced creation of adsorption sites and ion-induced chlorination:

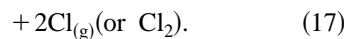
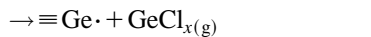
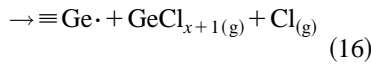
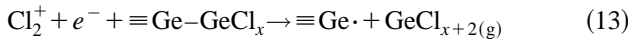
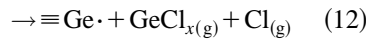
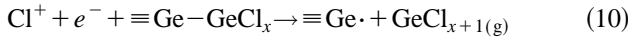


where e^- is an electron from the bulk.

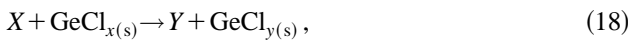
Neutral (or ion) chlorination:



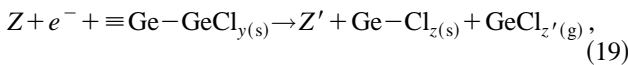
Ion-induced sputtering of GeCl_x :



Since the same chlorine content of the GeCl_x adlayer was measured for high ion current/fast etch conditions (bright mode) and low ion current/slow etch conditions (dim mode), both the adlayer chlorine content and the etch rate seem to be controlled by the ion current to the wafer. While many of these 17 steps are expected to be significant, it is not possible to determine their relative importance in this investigation. In a simplified model, which summarizes several features of reactions (1)–(9), chlorination occurs by



where $X = \text{Cl}, \text{Cl}_2, \text{Cl}^+, \text{ or } \text{Cl}_2^+$; $x = 0, 1, 2, \text{ or } 3$; $Y = \text{Cl}, \text{Cl}^+, \text{ or no species}$; and $y = 1, 2, 3, \text{ or } 4$. Similarly, the ion-induced sputtering reactions are summarized by



where $Z = \text{Cl}^+ \text{ or } \text{Cl}_2^+$ and $Z' = \text{Cl}, \text{Cl}_2, \text{ or no species}$.

The etch yield can be computed from Eqs. (18) and (19) using the etch rate, LD-LIF intensity, and ion flux measurements. Steady-state analysis of reactions (18) and (19) leads to the surface chlorination θ_{Cl} . Reaction (19) gives the ion-enhanced etch rate (ER) ($\text{atoms cm}^{-2} \text{ s}^{-1}$):

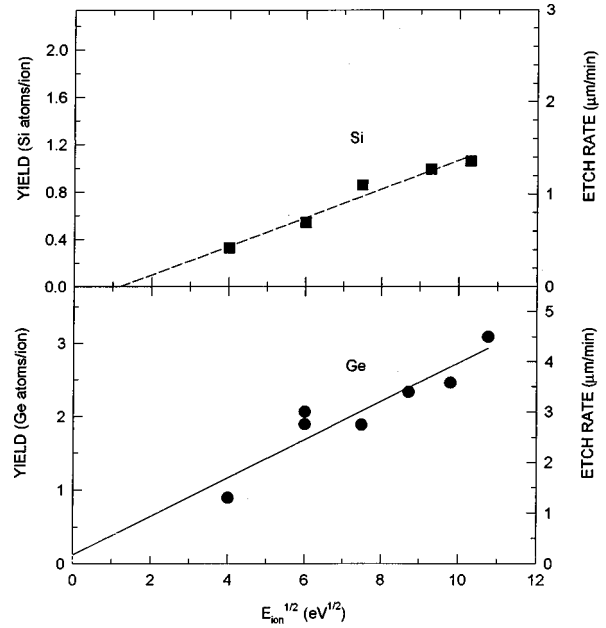


FIG. 11. Solid and the dashed curves are the least square fit to Eqs. (19) and (20) for the sputter yield of Ge and Si, respectively, vs the square root of ion energy. The etch rates of Ge (●) and Si (■) are also plotted for reference.

$$\text{ER} = \Phi_{\text{ion}} \tilde{Y}(E_{\text{ion}}, \theta_{\text{Cl}}) \propto \theta_{\text{Cl}} \Phi_{\text{ion}} Y(E_{\text{ion}}), \quad (20)$$

where Φ_{ion} is the flux of ions, $Y(E_{\text{ion}})$ is the yield at constant Cl coverage, and E_{ion} is the ion energy. E_{ion} is assumed to be equal to the plasma potential (16 V) plus the magnitude of the dc bias voltage. Steinbrüchel²⁴ has reported the following sputtering yield expression for low ion energy:

$$Y(E_{\text{ion}}) \approx A(E_{\text{ion}}^{1/2} - E_{\text{th}}^{1/2}), \quad (21)$$

where E_{th} is the threshold energy and A is a proportionality constant. Figure 11 shows good agreement for the least squares fit of the etch yield Y for Ge with $E_{\text{ion}}^{1/2}$ when plotted using Eq. (20) with a constant θ_{Cl} (saturation). The LD-LIF and supporting XPS measurements indeed show that θ_{Cl} is independent of ion energy for Ge etching. Langmuir probe measurements reported in Ref. 11 showed that the ion flux does not vary with ion energy, as expected. Figure 11 shows that the yield for Ge increases from ~ 1 atom/ion at 16 eV to ~ 3 atoms/ion at 116 eV.

For comparison, Fig. 11 also plots the etch rate and yield for Si etching in this same ICP using data presented in Ref. 11. The etch yield for Ge is about three times larger than that for Si. The yield Y has been plotted assuming that θ_{Cl} is independent of E_{ion} ; it increases from ~ 0.33 atoms/ion at 16 eV to 1.05 atoms/ion at 106 eV—the same factor of ~ 3 increase as seen for Ge in this range of ion energy. However, in Refs. 10 and 11 it was shown that θ_{Cl} increases with ion energy by a factor of ~ 1.8 for Si etching in the range plotted. In Ref. 22 it was demonstrated that much of this increase can be attributed to subsurface Cl, which is up to $\sim 20 \text{ \AA}$ deep in the surface. Using this variation of $\theta_{\text{Cl}}(E_{\text{ion}})$ in Eq. (20), Y increases only by a factor of ~ 1.8 from 16 to 106 eV for Si if the incident ions sputter subsurface chlorine as effi-

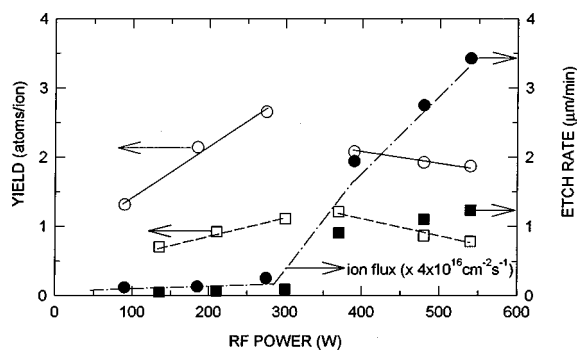


Fig. 12. Sputter yield of Ge (○) and Si (□) vs rf power [18 mTorr, -40 V dc bias (56 eV ion energy)]. The etch rates of Ge (●) and Si (■) and the ion flux (alternating dot-dashed curve) are also plotted for reference.

ciently as they do surface-bound chlorine. If this is not the case, the dependence of Y plotted in Fig. 11 is more accurate.

The extrapolated yield fits in Fig. 11 suggest that the threshold energy for Ge is near zero, while that for Si is about 1.4 eV. In a previous study of Si etching in a helical resonator,¹⁰ E_{th} was also found to be near zero. For comparison, note that the reported value of the threshold energy for Si is ~ 20 eV during $\text{Cl}-\text{Cl}^+$ beam etching^{25,26} and 25 eV during $\text{Cl}_2-\text{Cl}_2^+$ beam etching.²⁷ Perhaps the surface binding energies of volatile products are lower in a real high charge density plasma (ICP, HR) than those formed in such “simulated” ion-beam-etching type experiments, because the ion flux is much larger ($>4 \times 10^{16} \text{ cm}^{-2} \text{ s}^{-1}$) than that used in the ion beam etching experiments ($<1 \times 10^{16} \text{ cm}^{-2} \text{ s}^{-1}$) or the ratio of neutrals flux to ion flux is much higher.

Figure 12 plots the etch rate and yield versus rf power for Ge and Si, the latter plotted using data from Ref. 11. The measurement of Φ_{ion} with rf power reported in Ref. 11 is used to determine the yields. θ_{Cl} shows no systematic variation with rf power for either Ge or Si etching (and that θ_{Cl} is also the same for dim- and bright-mode operation). The ion yield is roughly 2 Ge atoms/ion and 0.8 Si atoms/ion at 56 eV ion energy, and these yields are both fairly independent of rf power. While this may not seem surprising, in ways it is remarkable because of the larger variation of plasma conditions over this range of rf power. There is an order of magnitude increase in ion flux from dim- to bright-mode operation, as well as a linear increase of flux with power within each mode. In dim-mode operation, Cl_2 is largely undissociated, while in bright-mode operation Cl_2 is increasingly dissociated into Cl, with $\sim 80\%$ – 90% of the Cl_2 dissociated at 600 W. Cl_2^+ is the dominant ion in dim-mode operation, while it is not clear whether Cl^+ or Cl_2^+ is dominant in bright-mode operation—both may be important. It is not clear whether the plotted variations of yield with rf power are real or (as seems more likely) are due to uncertainties in experimental parameters.

The threshold energy for Ge appears to be lower than that of Si. Even though this small difference (<2 eV) is within experimental uncertainty, it may be significant and may indicate that the binding energy for GeCl_x on Ge is lower than that for SiCl_x on Si. No etch yield analysis of Ge in a chlo-

rine plasma environment has been previously reported. In a temperature-programmed desorption study of a Cl-covered Si(111) surface, SiCl_2 desorbed at 950 K when the substrate was heated at 9 K/s (both at initial low and saturation coverage).²⁸ Similar results were obtained for a Cl-covered Si(100) surface when the substrate was heated at 5 K/s.²⁹ The activation energy of the desorption of SiCl_2 , assuming second-order kinetics, was 71–73 kcal/mol,^{28,29} which corresponds to ~ 3 eV per molecule. In contrast, GeCl_2 desorbed at 675 K when a Ge(100) surface exposed to HCl was heated at 2 K/s.¹⁹ This peak temperature for GeCl_2 desorption remained at 675 K (to within 10 K) for initial HCl coverages between 0.03 and 0.5 ML (saturation); the kinetics of desorption was assigned to be near first order. No desorption activation energy of GeCl_2 was reported. These results suggest that for thermally prepared surfaces the desorption activation energy of GeCl_2 is lower than that of SiCl_2 . Consequently, the surface binding energy and, consequently, the threshold yield energy for GeCl are presumably lower than those for SiCl for plasma-exposed surfaces.

Physical sputter etching studies of Ge and Si by inert gas ions such as Ar^+ support the ion-enhanced etching mechanism suggested by this study. Ar^+ ions (200 eV ion energy, 1 mA/cm² ion current density) sputter etch Ge (490 Å/min, giving Ge atoms) $3 \times$ faster than Si (160 Å/min, giving Si atoms).³⁰ This factor of 3 is also found in the reported studies of chlorine ions incident on chlorinated Ge and Si surfaces, giving GeCl and SiCl, in the ICP. This faster sputter etching for Ge than for Si suggests the relative ease of substrate attack for bond breaking by incoming ions for Ge compared to Si.

V. CONCLUSIONS

Laser desorption of the GeCl_x surface adlayer followed by laser-induced fluorescence detection of desorbed GeCl has been used to measure the degree of chlorination of the adlayer during Ge etching in a Cl_2 ICP reactor. The Ge surface is twice as chlorinated during ICP etching as it is during exposure to chlorine with the plasma off. Wait and probe measurements have shown that this GeCl_x adlayer is quite stable. The steady-state GeCl_x coverage increases rapidly to a saturation level, even at very low rf power (within 0.1 s at ~ 100 W) and is independent of rf power up to 600 W. At the same low power, the SiCl_x adlayer that forms during Si etching takes much longer (~ 5 s) to reach steady state.

The chlorine content of the adlayer is insensitive to the dc substrate bias (0 to -100 V), and consequently to the ion energy (16–116 eV) during Ge etching; this was confirmed by XPS analysis in a helical resonator. In contrast, the adlayer becomes more highly chlorinated with increasing dc bias during Si etching. It is unlikely that increasing ion energy leads to even deeper penetration of chlorine into the subsurface in Si but not in Ge. Perhaps the Ge subsurface is more easily attacked by ions than Si to provide extra sites for chlorination even at low bias, and bombardment by high ion energy (or fluxes) both enhances sputtering and steady-state chlorination during Ge etching. Etch yield analysis showed

that the etch yield of Ge increases from ~ 1 to 3 atoms/ion over this ion energy range, which is about $3\times$ that for Si. Ge appears to have a lower threshold energy for ion etching than Si during Cl_2 plasma etching.

Since the etch rate closely follows the ion current as the rf power is changed while the chlorine content of the adlayer does not change with power, the ion current to the wafer controls both the etch rate and the chlorine content of the adlayer; this has also been seen for Si etching.

ACKNOWLEDGMENTS

This work was supported by NSF Grant No. DMR-94-11504. The authors would like to thank Bing C. Wang and Jonathan Spanier for assistance in conducting the experiments.

¹A. A. Bright, S. S. Iyer, S. W. Robey, and S. L. Delage, *Appl. Phys. Lett.* **53**, 2328 (1988).

²S. W. Robey, A. A. Bright, G. S. Oehrlein, S. S. Iyer, and S. L. Delage, *J. Vac. Sci. Technol. B* **6**, 1650 (1988).

³G. S. Oehrlein, Y. Zhang, G. M. W. Kroesen, E. de Fresart, and T. D. Bestwick, *Appl. Phys. Lett.* **58**, 2252 (1991).

⁴G. S. Oehrlein, T. D. Bestwick, P. L. Jones, M. A. Jaso, and J. L. Lindstrom, *J. Electrochem. Soc.* **138**, 1443 (1991).

⁵Y. Zhang, G. S. Oehrlein, and E. de Fresart, *J. Appl. Phys.* **71**, 1936 (1992).

⁶Y. Kuo, *Mater. Res. Soc. Symp. Proc.* **316**, 1041 (1994).

⁷M. C. Peignon, Ch. Cardinaud, G. Turban, C. Charles, and R. W. Boswell, *J. Vac. Sci. Technol. A* **14**, 156 (1996).

⁸G. F. McLane, M. Dubey, M. C. Wood, and K. E. Lynch, *J. Vac. Sci. Technol. B* **15**, 990 (1997).

⁹I. P. Herman, V. M. Donnelly, K. V. Guinn, and C. C. Cheng, *Phys. Rev. Lett.* **72**, 2801 (1994).

¹⁰C. C. Cheng, K. V. Guinn, V. M. Donnelly, and I. P. Herman, *J. Vac. Sci. Technol. A* **12**, 2630 (1994).

¹¹J. Y. Choe, I. P. Herman, and V. M. Donnelly, *J. Vac. Sci. Technol. A* **15**, 3024 (1997).

¹²C. C. Cheng, K. V. Guinn, I. P. Herman, and V. M. Donnelly, *J. Vac. Sci. Technol. A* **13**, 1970 (1995).

¹³R. W. B. Pearse and A. G. Gaydon, *The Identification of Molecular Spectra*, 4th ed. (Chapman and Hall, London, 1976), p. 164.

¹⁴W. Jevons, L. A. Bashford, and H. V. A. Briscoe, *Proc. Phys. Soc. London* **49**, 532 (1937).

¹⁵A. P. Filippova and Yu. Ya. Kuzyakov, *Vestn. Mosk. Univ., Ser. II: Khim.* **3**, 25 (1968).

¹⁶G. A. Oldershaw and K. Robinson, *Trans. Faraday Soc.* **66**, 532 (1970).

¹⁷R. D. Schnell, F. J. Himpsel, A. Bogen, D. Rieger, and W. Steinmann, *Phys. Rev. B* **32**, 8052 (1985).

¹⁸R. J. Madix and J. A. Schwarz, *Surf. Sci.* **24**, 264 (1971).

¹⁹M. P. D'Evelyn, Y. L. Yang, and S. M. Cohen, *J. Chem. Phys.* **101**, 2463 (1994).

²⁰Q. Z. Qin, Y. L. Li, P. H. Lu, Z. J. Zhang, Z. K. Jin, and Q. K. Zheng, *J. Vac. Sci. Technol. B* **10**, 201 (1992).

²¹V. M. Donnelly (unpublished results).

²²N. Layadi, V. M. Donnelly, and J. T. C. Lee, *J. Appl. Phys.* **81**, 6738 (1997).

²³S. Vallon, C. Monget, O. Joubert, L. Vallier, F. H. Bell, M. Pons, J. L. Regolini, C. Morin, and I. Sagnes, *J. Vac. Sci. Technol. A* **14**, 1874 (1997).

²⁴C. Steinbrüchel, *Appl. Phys. Lett.* **55**, 1960 (1989).

²⁵J. P. Chang and H. H. Sawin, *J. Vac. Sci. Technol. A* **15**, 610 (1997).

²⁶J. P. Chang, A. P. Mahorowala, and H. H. Sawin, *J. Vac. Sci. Technol. A* **16**, 217 (1998).

²⁷M. Balooch, M. Moalem, W.-E. Wang, and A. V. Hamza, *J. Vac. Sci. Technol. A* **14**, 229 (1996).

²⁸P. Gupta, P. A. Coon, B. G. Koehler, and S. M. George, *Surf. Sci.* **249**, 92 (1991).

²⁹M. A. Mendicino and E. G. Seebauer, *Appl. Surf. Sci.* **68**, 285 (1993).

³⁰P. R. Puckett, S. L. Michel, and W. E. Hughes, in *Thin Film Processes II*, edited by J. Vossen and W. Kern (Academic, San Diego, 1991), p. 758.